Progress In Electromagnetics Research B, Vol. 19, 285–303, 2010

NOVEL METHOD TO ANALYZE AND DESIGN ONE-DIMENSIONAL RECIPROCAL PERIODIC STRUCTURES WITH SYMMETRICAL CELLS

O. Zandi and Z. Atlasbaf

Department of Electrical and Computer Engineering
Tarbiat Modares University
Tehran, Iran

M. S. Abrishamian

Department of Electrical Engineering
K.N. Toosi University of Technology
Tehran, Iran

Abstract—The dispersion relation is derived for the most general configuration of a passive and reciprocal periodically loaded transmission line in a unique and simple form by introducing two novel parameters. Based on this relation, the phase and group velocities are determined and a simple condition for phase reversal propagation is obtained. The two above mentioned parameters help us to develop a polar diagram to model the behavior of any two-port network as a function of frequency. By this diagram, we can determine the direction of the phase velocity and also the value of the propagation constant. Then, symmetrical cells and thereof the periodic structures composed of them are analyzed. For such structures, it will be shown that the dispersion relation can be rewritten in a form similar to the Lorentz transformation. We design and analyze a bandstop filter to verify the method.

1. INTRODUCTION

Theory of periodic structures is one of the most adequate methods to analyze and design artificial structures. Frequency selective surfaces [1, 2], electromagnetic band-gap (EBG) structures [3, 4], microwave filters [5], phase reversal or left-handed transmission lines [6] etc., are some fields where this theory can be used.

Corresponding author: O. Zandi (omid_zandi@modares.ac.ir).

We consider a 1-dimensional (1-D) periodic structure which is made of identical cells that are separated by transmission lines of equal lengths. In order to analyze it, the basic and prevalent idea is to analyze the smallest piece of the structure which is periodically repeated and then generalize the results to the whole structure by using the Floquet's theory [5, 7]. Obviously the method is accurate for infinitely long structures. In fact, reducing the number of cells decreases the accuracy. Therefore efficient numerical methods should be used like the method of moments [8, 9], finite difference time domain [3, 10] etc. A periodic structure is large enough when the Bloch impedance concept [5, 7] can be used to calculate the reflection coefficient from a terminating load with sufficient accuracy.

In this paper, the transmission matrix for π or T model of the cells will be used to obtain the dispersion relation. Thereafter, we shall move into another space — we call it '*tardiness space*' — wherein the results will be simplified. For example, the dispersion relation gets a unique and simple form where the cells equivalent circuit elements won't appear explicitly in it.

In the mentioned space, it will be much easier to derive compact formulas for the phase and group velocities functions. The signs of these functions are determined and used to find a general condition for phase reversal propagation. A polar diagram is developed which shows the tardiness space parameters and helps to determine the value of the propagation constant and the directions of the phase and group velocities geometrically. Hence, working with this diagram is preferred to the Smith chart [11].

When considering the cells with symmetrical characteristics, one observes that the dispersion relation is very similar to the Lorentz transformation in the theory of special relativity or the wavelength relation in rectangular waveguides.

To show how the method works, we propose a systematic method to design symmetrical cells. The reflection coefficient of an isolated symmetrical cell will be derived first in the tardiness space and second by using the method of small reflections [5]. By comparing these two equations, we shall get a significant insight into the problem. Finally, a microstrip bandstop filter will be designed by tardiness space parameters. The results are verified by a full wave simulation.

2. DISPERSION RELATION OF A PERIODICALLY LOADED TRANSMISSION LINE

Figure 1 shows the most general forms of a passive and reciprocal 1-D periodic structure: π and T equivalent circuits of the cells separated

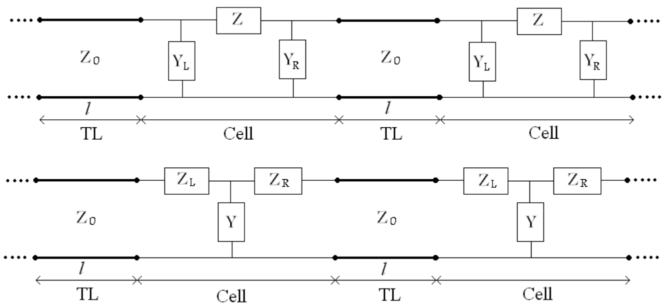

Figure 1. π and T models of cells loaded periodically in a transmission line.

by transmission lines of physical length l and characteristic impedance $Z_0 = 1/Y_0$.

If $[A\ B; C\ D]$ is the transmission matrix, the dispersion relation can be written as [5, 7]

$$\cosh(\alpha l + j\beta l) = (A + D)/2 \tag{1}$$

where α and β are the attenuation and the propagation constants respectively. The value of $(A + D)/2$ for π and T circuits are:

$$\begin{aligned}\frac{A_\pi + D_\pi}{2} &= \frac{2 + (Y_R + Y_L)\, Z}{2} \cos k_0 l \\ &\quad + j\frac{1}{2Y_0}\left(Y_R + Y_L + Y_R Y_L Z + \frac{Z}{Z_0^2}\right) \sin k_0 l \end{aligned} \tag{2a}$$

$$\begin{aligned}\frac{A_T + D_T}{2} &= \frac{2 + (Z_R + Z_L)\, Y}{2} \cos k_0 l \\ &\quad + \frac{j}{2Z_0}\left(Z_R + Z_L + Z_R Z_L Y + Z_0^2 Y\right) \sin k_0 l \end{aligned} \tag{2b}$$

k_0 is the propagation constant in an unloaded line. If we insert either (2a) or (2b) into (1), we will find that the obtained equation has the form of

$$\cosh(\alpha l + j\beta l) = r(\omega) \cos(k_0 l - \theta(\omega)) \tag{3a}$$

where

$$r\,(\omega) = \sqrt{\xi^2 + \zeta^2}, \quad \theta\,(\omega) = \tan^{-1}\,(\zeta/\xi) \tag{3b}$$

and

$$\begin{aligned} \xi &= \begin{cases} \frac{2+(Y_R+Y_L)Z}{2} & \text{For } \pi \text{ model} \\ \frac{2+(Z_R+Z_L)Y}{2} & \text{For T model} \end{cases} \\ \zeta &= \begin{cases} \frac{j}{2Y_0}\left(Y_R + Y_L + Y_R Y_L Z + Y_0^2 Z\right) & \text{For } \pi \text{ model} \\ \frac{j}{2Z_0}\left(Z_R + Z_L + Z_R Z_L Y + Z_0^2 Y\right) & \text{For T model} \end{cases} \end{aligned} \tag{3c}$$

Since the impedances and admittances in (3c) can be functions of frequency, we write r and θ as functions of ω. (Note that they can also be functions of voltages and/or currents if the structure is not linear but here linearity is presumed.) We call r and θ the *tardiness radius* and the *tardiness direction* or *angle* respectively. Eq. (3a) is a general form of the dispersion relation.

We assume that the cells and the transmission lines are lossless, therefore ξ and ζ both will be real and so are r and θ. In this case only one of the two parameters α and β will be nonzero.

3. PHASE AND GROUP VELOCITIES

Our second assumption is that the structure is working in its pass band so $\alpha = 0$ but $\beta \neq 0$. For normalized phase velocity according to its definition [5, 7] and from (3a) we have

$$\frac{v_p}{c} = \frac{1}{c}\frac{\omega}{\beta} = \frac{k_0 l}{\beta l} = \pm \frac{k_0 l}{\cos^{-1}\left[r(\omega)\cos\left(k_0 l - \theta(\omega)\right)\right]} \tag{4}$$

where c is the propagation velocity in an *unloaded line* and $k_0 = \omega/c$. The $\pm$ sign is due to the inverse cosine function. The poles of phase velocity can be determined by:

$$\cos\left(\frac{l}{c}\omega_{pp} - \theta(\omega_{pp})\right) = 1/r(\omega_{pp}) \tag{5}$$

If $r(\omega)$ is larger than unity for some frequencies, the phase velocity may become imaginary.

To derive the normalized group velocity, we take derivative of both sides of (3a) with respect to $k_0 l$ and find

$$-\frac{d(\beta l)}{d(k_0 l)}\sin(\beta l) = \frac{c}{l}\frac{dr(\omega)}{d\omega}\cos(k_0 l - \theta(\omega)) - r(\omega)\left[1 - \frac{c}{l}\frac{d\theta(\omega)}{d\omega}\right]\sin(k_0 l - \theta(\omega)) \tag{6}$$

Now from the definition of the group velocity [5, 7] we have

$$\begin{aligned}\frac{v_g}{c} &= \frac{1}{c}\frac{d\omega}{d\beta} = \frac{d(k_0 l)}{d(\beta l)} \\ &\quad \frac{\pm\sqrt{1 - r^2(\omega)\cos^2(k_0 l - \theta(\omega))}}{r(\omega)\left[1 - \frac{c}{l}\frac{d\theta(\omega)}{d\omega}\right]\sin(k_0 l - \theta(\omega)) - \frac{c}{l}\frac{dr(\omega)}{d\omega}\cos(k_0 l - \theta(\omega))}\end{aligned} \tag{7}$$

The $\pm$ sign is due to the root square function in the numerator. Poles of the phase velocity are zeros of the group velocity. Also the phase and group velocities are both imaginary in cutoff bands. The poles of the group velocity can be determined by:

$$\tan\left(k_0 l - \theta\left(\omega_{gp}\right)\right) = \frac{c}{l}\frac{1}{r\left(\omega_{gp}\right)}\left.\frac{dr\left(\omega\right)}{d\omega}\right|_{\omega=\omega_{gp}} \times \frac{1}{1-\frac{c}{l}\left.\frac{d\theta(\omega)}{d\omega}\right|_{\omega=\omega_{gp}}} \tag{8}$$

Equations (4) and (7) are the most general expressions for the phase and the group velocities for 1-D periodic structures.

Since sine function is odd then multiplying (4) by (7) results in an expression with no $\pm$ sign therefore we have:

$$\begin{aligned}\frac{v_p v_g}{c^2} &= \frac{k_0 l\sqrt{1-r^2\left(\omega\right)\cos^2\left(k_0 l-\theta\left(\omega\right)\right)}}{\cos^{-1}\left[r\left(\omega\right)\cos\left(k_0 l-\theta\left(\omega\right)\right)\right]} \\ &\times\frac{1}{r(\omega)\left[1-\frac{c}{l}\frac{d\theta(\omega)}{d\omega}\right]\sin(k_0 l-\theta\left(\omega\right))-\frac{c}{l}\frac{dr(\omega)}{d\omega}\cos(k_0 l-\theta\left(\omega\right))}\end{aligned} \tag{9}$$

It is evident that if ω_{gp} is an odd order pole, the sign of $v_p v_g$ will change whenever the angular frequency passes it.

It is worth mentioning that between any two successive poles there are two sets of frequency bands. In one of them, the normalized group velocity is greater than unity which is not acceptable. It represents a kind of anomalous dispersion bands, i.e., when a group of signals with different frequencies passes through them, it will be disturbed [12]. Clearly these bands are not restricted to areas around the poles. The other set refers to ordinary propagations.

4. INTERPRETATION OF THE TARDINESS RADIUS AND DIRECTION

Let us consider the simplest case where in the considered frequency band we have

$$dr(\omega)/d\omega = 0 \Rightarrow r(\omega) = r_0 \quad d\theta(\omega)/d\omega = 0 \Rightarrow \theta(\omega) = \theta_0 \tag{10}$$

So (4) and (7) reduce to

$$\frac{v_p}{c} = \pm\frac{k_0 l}{\cos^{-1}\left[r_0\cos\left(k_0 l-\theta_0\right)\right]} \tag{11a}$$

$$\frac{v_g}{c} = \pm\frac{\sqrt{1-r_0^2\cos^2\left(k_0 l-\theta_0\right)}}{r_0\sin\left(k_0 l-\theta_0\right)} \tag{11b}$$

and (9) becomes

$$\frac{1}{c^2}v_p v_g = \frac{k_0 l\sqrt{1-r_0^2\cos^2\left(k_0 l-\theta_0\right)}}{r_0\sin\left(k_0 l-\theta_0\right)\cos^{-1}\left[r_0\cos\left(k_0 l-\theta_0\right)\right]} \tag{12}$$

Equations (11a) and (11b) show the periodic nature of the phase and the group velocities with respect to the frequency. From (11b), the anomalous dispersion region is $r_0 < 1$. $r_0 = 1$ corresponds to an unloaded line. Figure 2 shows these three functions for two values of r_0 and two values of θ_0 versus $k_0 l$. Increasing the value of r_0 decreases the bandwidth and the group velocity, i.e., it retards the propagation. On the other hand, changing the value of θ_0 may change the direction of phase velocity in contrast to the group velocity which is assumed to be in the outward direction of the source. Due to (12) and the discussions in the previous section, phase reversal occurs whenever

$$\sin\left(k_0 l - \theta_0\right) < 0 \tag{13}$$

Now the group velocity in (7) can be rewritten as

$$\frac{v_g}{c} = \pm \frac{1}{\Pi\left(\omega\right)} \frac{\sqrt{1 - r^2\left(\omega\right)\cos^2\left(k_0 l - \theta\left(\omega\right)\right)}}{r\left(\omega\right)\left[\sin\left(k_0 l - \theta\left(\omega\right) - \Psi\left(\omega\right)\right)\right]} \tag{14}$$

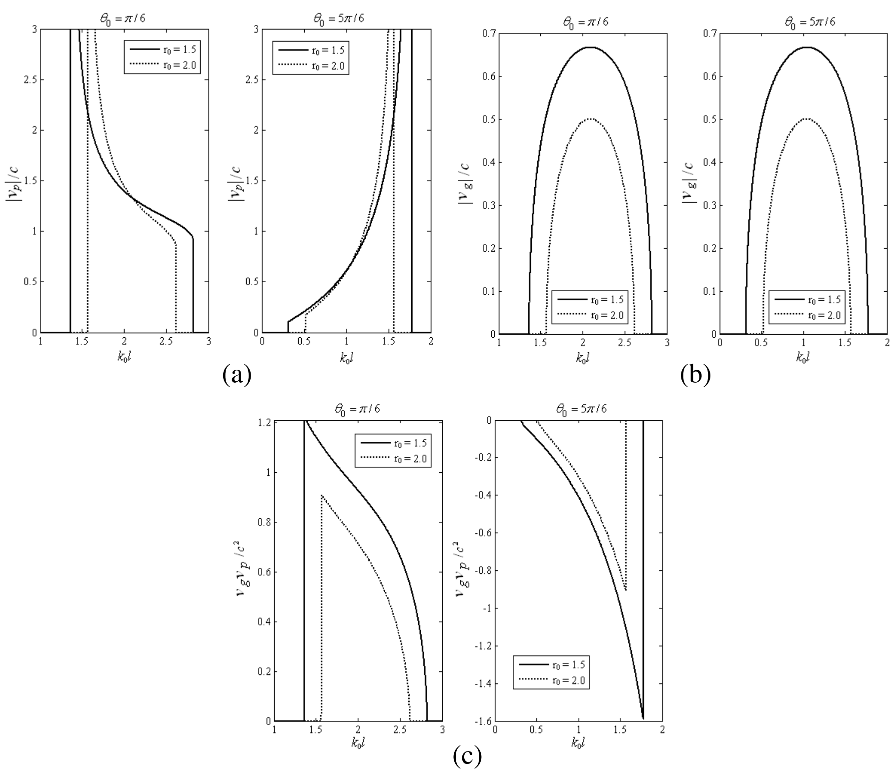

Figure 2. (a) Normalized phase velocity, (b) normalized group velocity and (c) their multiplication versus $k_0 l$.

where

$$\Psi(\omega) = \tan^{-1}\left[\frac{1}{l/c - d\theta(\omega)/d\omega}\frac{1}{r(\omega)}\frac{dr(\omega)}{d\omega}\right] \tag{15a}$$

and

$$\Pi(\omega) = \left\{\left[1 - \frac{c}{l}\frac{d\theta(\omega)}{d\omega}\right]^2 + \left[\frac{c}{l}\frac{1}{r(\omega)}\frac{dr(\omega)}{d\omega}\right]^2\right\}^{1/2} \tag{15b}$$

The form of (14) is somehow similar to (11b). Phase reversal propagation condition is apparently

$$\sin(k_0 l - \theta(\omega) - \Psi(\omega)) < 0 \tag{16}$$

But the anomalous dispersion occurs whenever the numerator of (14) becomes greater than its denominator.

5. DESIGN PROCEDURE IN THE TARDINESS SPACE

All the design procedure can be based on (11a) and (11b) and is clearly depicted in Figure 3. At first one has to select the location of the initial point (r_0, θ_0) in the polar diagram. Then the operating point $(r_0, k_0 l - \theta_0)$ can be determine. At this stage, $\cos(\beta l)$ can be obtained which its absolute value must be less than unity in the pass band. For phase reversal propagation from (13) the following equation must be valid:

$$(2n-1)\pi < k_0 l - \theta_0 < 2n\pi$$

where n is an integer. To design a left-handed TL, one should choose $l < \lambda/4$ or $0 \leq k_0 l < \pi/2$ to satisfy the homogeneity condition [6]. Therefore the best choice of θ_0 seems to be in the second quarter with an appropriate value of r_0.

For a desired bandwidth the value of r_0 will be selected. In a real design, the tardiness radius and direction will be functions of frequency, so the operating point do not remain on a constant radius circle when the frequency changes.

Henceforth, we restrict the subject to symmetrical cells shown in Figure 4. Using (3c), we determine the shunt admittances ($Y_R = Y_L = Y_\pi$) and the series impedance (Z_π) for the π model as:

$$Y_\pi^{sh} = jY_0 \frac{-r\sin\theta \pm \sqrt{r^2-1}}{r\cos\theta + 1} \tag{17a}$$

$$Z_\pi^{se} = \frac{1}{jY_0}\frac{r^2\cos^2\theta - 1}{-r\sin\theta \pm \sqrt{r^2-1}} \tag{17b}$$

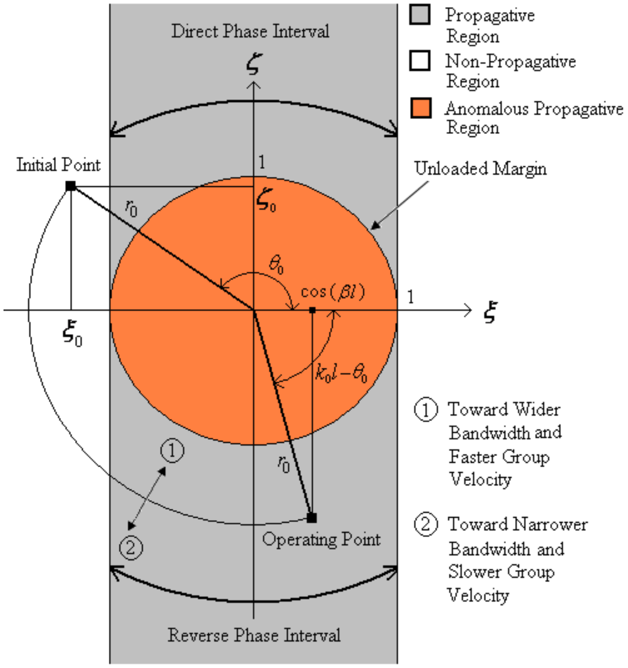

Figure 3. Tardiness space for a passive and reciprocal periodically loaded transmission line.

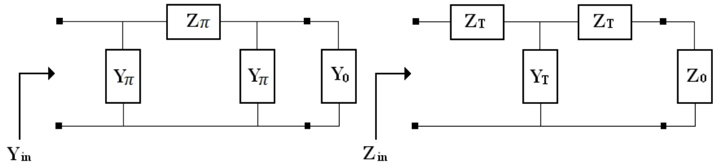

Figure 4. Isolated symmetrical π or T cell between transmission lines.

And for the T model the series impedances ($Z_R = Z_L = Z_T$) and the shunt admittance (Y_T) as:

$$Z_T^{se} = jZ_0 \frac{-r \sin\theta \pm \sqrt{r^2 - 1}}{r \cos\theta + 1} \tag{18a}$$

$$Y_T^{sh} = \frac{1}{jZ_0} \frac{r^2 \cos^2\theta - 1}{-r \sin\theta \pm \sqrt{r^2 - 1}} \tag{18b}$$

Another parameter which should be found in terms of r and θ, is the reflection coefficient from an isolated cell inserted in between transmission lines Γ_c. To calculate Γ_c, we determine the input impedance or admittance which is shown in Figure 4 as:

$$\frac{Y_{in}^{\pi}}{Y_0} = \frac{(r\cos\theta + 1)\frac{Y_{\pi}^{sh}}{Y_0} + r\cos\theta}{r\cos\theta + Z_{\pi}^{se}Y_0} \tag{19a}$$

$$\frac{Z_{in}^{T}}{Z_0} = \frac{(r\cos\theta + 1)\frac{Z_{T}^{se}}{Z_0} + r\cos\theta}{r\cos\theta + Y_{T}^{sh}Z_0} \tag{19b}$$

So we have:

$$\Gamma_c^{\pi} = (1 - Y_{in}^{\pi}/Y_0)/(1 + Y_{in}^{\pi}/Y_0), \quad \Gamma_c^{T} = \left(Z_{in}^{T}/Z_0 - 1\right)/\left(Z_{in}^{T}/Z_0 + 1\right) \tag{20}$$

If we insert (19) into (20), we will find:

$$|\Gamma_c| = \sqrt{1 - 1/r^2} \tag{21a}$$

Or inversely

$$r = 1/\sqrt{1 - |\Gamma_c|^2} \tag{21b}$$

Figure 5 shows the absolute value of reflection coefficient versus r.

Also the phase of the reflection coefficient in (20) is independent of r and just depends on θ. We have:

$$\angle\Gamma_c = \begin{cases} \theta \mp \pi/2 & \pi\,\text{Model} \\ \theta \pm \pi/2 & \text{T Model} \end{cases} \tag{21c}$$

where plus-minus signs are the same as what has appeared in (17) or (18).

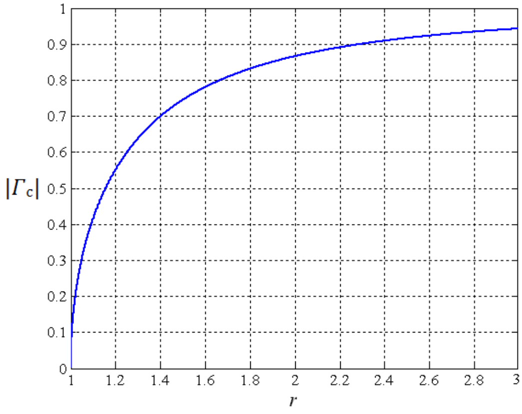

Figure 5. The absolute value of reflection coefficient versus r.

By inserting (21b) and (21c) into the dispersion relation (3a), one will find that for π model

$$\cos(\beta l) = \mp \sin(k_0 l - \angle\Gamma_c) / \sqrt{1 - |\Gamma_c|^2} \tag{22}$$

and for the T model, the minus-plus sign should be replaced by $\pm$.

Now the design procedure is complete. We use the reflection coefficient from an isolated cell rather than its equivalent circuit. Both the analytical and numerical methods would be helpful.

To terminate a periodic structure in a load, the Bloch impedance [5, 7] Z_B must be known. For symmetrical cells and T model it is given by the following expressions

$$\begin{aligned} Z_B &= \pm Z_0 \frac{\sqrt{1 - r^2\cos^2(k_0 l - \theta)}}{r\sin(k_0 l - \theta) + r\sin\theta + \frac{r^2\cos^2\theta - 1}{-r\sin\theta \pm \sqrt{r^2-1}}} \\ &= \pm Z_0 \frac{r\sin(k_0 l - \theta) - r\sin\theta - \frac{r^2\cos^2\theta - 1}{-r\sin\theta \pm \sqrt{r^2-1}}}{\sqrt{1 - r^2\cos^2(k_0 l - \theta)}} \end{aligned} \tag{23}$$

6. SYMMETRICAL CELLS

A symmetrical cell among a microstrip or waveguide line is shown in Figure 6. As it can be seen, the width of the line is a function of position.

The line is in x direction. The cell's physical length is S and its center is at $x = 0$. If the characteristic impedance in the interval of $0 \le x \le S/2$ is $Z_c(x)$, the reflection coefficient can be found by the method of small reflections as [13]:

$$\Gamma_S = -j\exp\left(-2j\int_0^{S/2} k(x')\,dx'\right)\int_0^{S/2} \sin\left(2\int_0^{x} k(x')\,dx'\right)\frac{Z_c'(x)}{Z_c(x)}dx \tag{24}$$

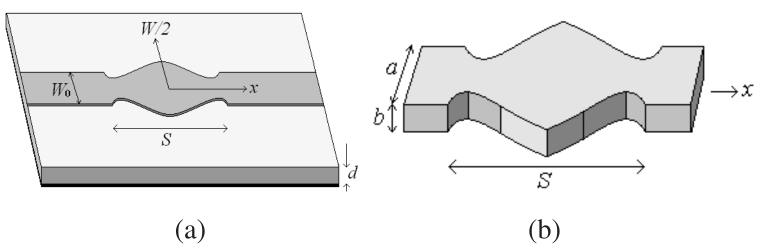

Figure 6. A symmetrical cell among (a) a microstrip, (b) a waveguide transmission line.

where $Z'_c(x) = dZ_c(x)/dx$. $k(x)$ is the propagation constant in the cell. Eq. (24) is a general relation for any symmetrical cell and is valid if $Z_c(x)$ is a continuous and well-behaved function.

Equation (24) suggests that a symmetrical cell is a combination of a transmission line of length l:

$$l = (2/k_0) \int_0^{S/2} k\,(x)\,dx \tag{25a}$$

and a lumped element with the reflection coefficient as defined in (20), of

$$\Gamma_c = -j \int_0^{S/2} \sin\left(2\int_0^{x} k\left(x'\right) dx'\right) Z'_c\,(x)\,/Z_c\,(x)\,dx \tag{25b}$$

which its tardiness angle can be found using (21c) as

$$\theta_0 = 0 \text{ or } \pi \tag{25c}$$

Eqs. (22) and (25b) reveal that

$$|\cos\left(\beta l\right)| = \frac{|\cos\left(k_0 l\right)|}{\sqrt{1 - |\Gamma_c|^2}} \tag{26}$$

which is comparable to the Lorentz transformation or the wavelength relation in rectangular waveguides.

Let turn our attention on microstrip lines. The Taylor expansion of the propagation constant as a function of the line width can be determined from the analytical formulas [5]. We write

$$k = \frac{\omega}{c}\left[\bar{k}_0 + \bar{k}_1\,(W - W_0) + \bar{k}_2\,(W - W_0)^2 + \ldots\right] \tag{27}$$

where W_0 is the width of an unloaded line with characteristic impedance Z_0. c stands for the propagation velocity in *free space.* The expansion is around W_0 and the two first terms are:

$$\bar{k}_0 = \sqrt{\frac{(\varepsilon_r+1)\sqrt{1+12d/W_0}+\varepsilon_r-1}{2\sqrt{1+12d/W_0}}}, \quad \bar{k}_1 = \frac{3d\,(\varepsilon_r-1)}{2W_0^2\bar{k}_0\,(1+12d/W_0)^{3/2}} \tag{28}$$

where ε_r is the relative permittivity of the substrate and d is its thickness. We may consider the form of

$$W\,(x) = \sum_{n=0}^{N} W_n\,(x - S/2)^n \quad 0 \le x \le S/2 \tag{29}$$

for $W(x)$ which should be positive in the given interval. We could exert other constraints on $W(x)$ such as

$$dW(x)/dx|_{x=0} = dW(x)/dx|_{x=S/2} = 0, \quad W(0) = TW_0 \tag{30}$$

where $0.5 < T < 2.5$ is an arbitrary real number. So (29) for $N = 3$ gives

$$W_1 = 0, \quad W_2 = 12(T-1)W_0/S^2, \quad W_3 = 12(T-1)W_0/S^3 \tag{31}$$

This is an arbitrary choice and any other continuous and well-behaved function can be selected for W. Our proposed cell is shown in Figure 7.

Now we can determine the amplitude of the reflection coefficient in (24). Let's call it I:

$$I = j\Gamma_c$$
$$\approx \int_0^{S/2} \sin\left(\frac{2\omega}{c}\left[\bar{k}_0 x + \bar{k}_1 \sum_{n=1}^{N} W_n \left(\frac{(x-S/2)^{n+1}}{n+1} - \frac{(-S/2)^{n+1}}{n+1}\right)\right]\right) \frac{Z_c'(x)}{Z_c(x)} dx \tag{32}$$

where we have [5]:

$$Z_c(x) = \begin{cases} \frac{60}{\sqrt{\varepsilon_e}} \ln\left(\frac{8d}{W} + \frac{W}{4d}\right) & W/d \le 1 \\ \frac{120\pi d}{\sqrt{\varepsilon_e}[W+1.393d+0.667d[\ln(W+1.444d)-\ln d]]} & W/d \ge 1 \end{cases} \tag{33a}$$

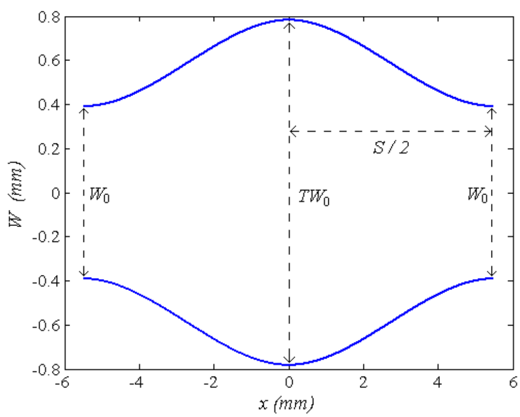

Figure 7. The geometry of proposed symmetrical microstrip cell.

and in turn it leads to

$$Z_c'(x) = -dW/dx$$
$$\times \begin{cases} \frac{d\varepsilon_e}{dW}\frac{30}{\varepsilon_e^{3/2}}\ln\left(\frac{8d}{W}+\frac{W}{4d}\right)+\frac{60}{\sqrt{\varepsilon_e}}\frac{32d^2-W^2}{W(32d^2+W^2)} & W/d\le 1 \\ \frac{d\varepsilon_e}{dW}\frac{60\pi d}{\varepsilon_e^{3/2}[W+1.393d+0.667d[\ln(W+1.444d)-\ln d]]} & \\ +\frac{120\pi d\left[1+\frac{0.667d}{W+1.444d}\right]}{\sqrt{\varepsilon_e}[W+1.393d+0.667d[\ln(W+1.444d)-\ln d]]^2} & W/d\ge 1 \end{cases} \tag{33b}$$

where

$$\frac{d\varepsilon_e}{dW} = \frac{3d(\varepsilon_r-1)}{W^2(1+12d/W)^{3/2}} \tag{33c}$$

We insert (33a) and (33b) into (32) and solve the integral numerically. The design parameters are:

$$\varepsilon_r = 2.2, \quad d = 0.01\,\text{inch}, \quad Z_0 = 50\,\Omega$$

I, generally is a function of T, S and the frequency as shown in Figure 8. T is restricted to lie in the interval of [0.5 2.5] where the Taylor expansion remains valid in (27).

To design a bandstop filter we choose $S = 1.1$ cm and $T = 2.0$ but how can we determine the bandwidth?

We should reemphasize that the tardiness radius is a function of frequency; hence we should determine its path in the tardiness diagram as the frequency changes. In Figure 9, I versus frequency in a very broad band (from zero to 50 GHz) is sketched. In Figure 10, the behavior of the designed structure is depicted in the tardiness space. The bandwidth is predicted as well. We see the cells enter

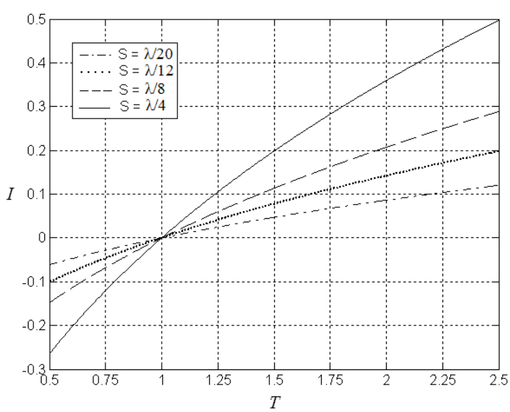

Figure 8. Amplitude of reflection coefficient versus T for three values of S. λ is the wave length of an unloaded line (i.e., $I = 0$).

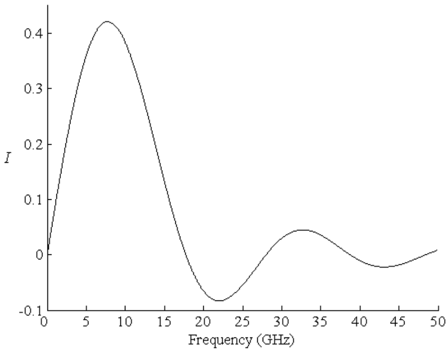

Figure 9. I versus frequency.

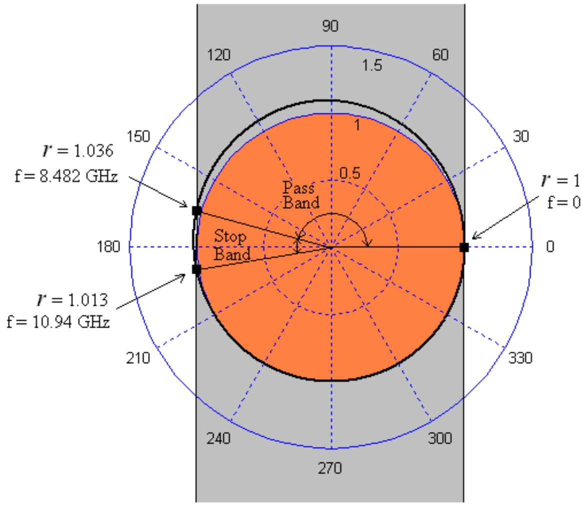

Figure 10. The behavior of the designed structure in tardiness space.

the phase reversal region at $f = 10.94\,\mathrm{GHz}$ but they do not satisfy the homogeneity condition. The reflection coefficient when the structure is terminated in a load Z_0, will be

$$\Gamma = (Z_B - Z_0)\,/\,(Z_B + Z_0) \tag{34}$$

where Z_B is the Bloch impedance in (23). Γ as a function of frequency is shown in Figure 11.

The equivalent T network series impedances and shunt admittance can be determined from (18a) and (18b). Due to plus-minus signs, two equivalent circuits are possible which are shown in Figure 12. In Figure 13, the values of inductances or capacitances are sketched versus frequency. As expected, the value of L_{sh} or C_{se} becomes infinite when the frequency approaches zero.

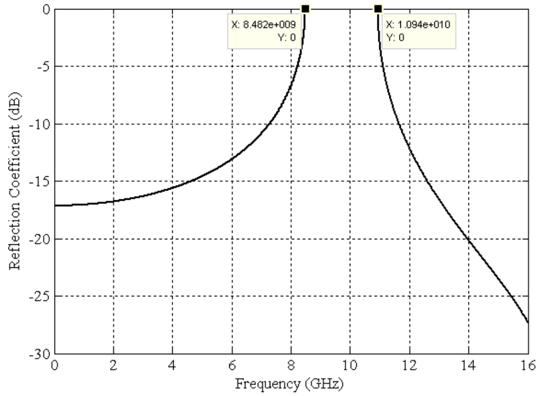

Figure 11. Reflection coefficient versus frequency obtained from the Bloch impedance.

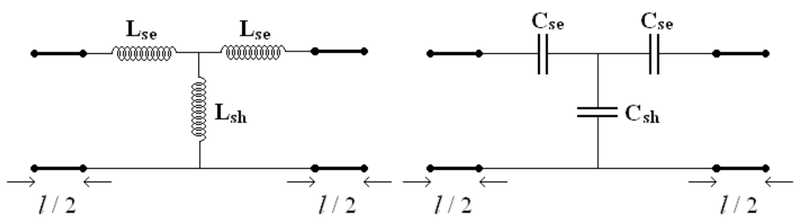

Figure 12. Two possible equivalent circuits of the symmetrical microstrip cell shown in Figure 7.

Interestingly the same problem has been solved for a rectangular waveguide with sinusoidally varying width but by another approach rather than the small reflections [14]. However, the results are the same.

7. SIMULATION

A periodic structure composed of five cells is simulated by HFSS. To compare it with the analytical method developed in this paper, we construct the total structures transmission matrix which is

$$\begin{bmatrix} A' & B' \\ C' & D' \end{bmatrix} = \begin{bmatrix} A & B \\ C & D \end{bmatrix}^5 \tag{35}$$

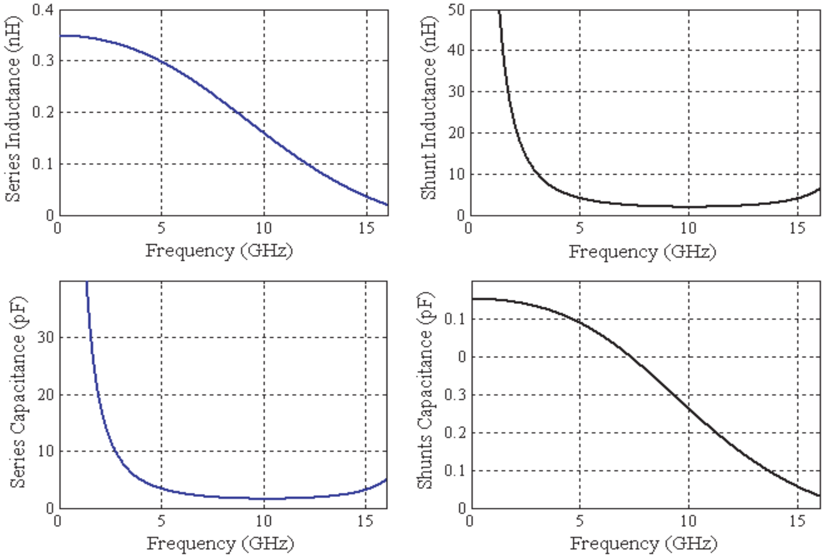

Figure 13. Series and shunt inductances and capacitances shown in two possible equivalent circuits in Figure 12.

where A, B, C and D return to a single cell and for a symmetrical T network are:

$$A_T = D_T = r\cos(k_0 l - \theta) \tag{36a}$$

$$B_T = jZ_0\left[r\sin(k_0 l - \theta) - r\sin\theta + \frac{r^2\cos^2\theta - 1}{-r\sin\theta \pm \sqrt{r^2-1}}\right] \tag{36b}$$

$$C_T = jY_0\left[r\sin(k_0 l - \theta) + r\sin\theta - \frac{r^2\cos^2\theta - 1}{-r\sin\theta \pm \sqrt{r^2-1}}\right] \tag{36c}$$

We have [5]

$$S_{11} = \frac{B'/Z_0 - C'Z_0}{2A' + B'/Z_0 + C'Z_0} \tag{37a}$$

$$S_{12} = \frac{2}{2A' + B'/Z_0 + C'Z_0} \tag{37b}$$

Scheme of the structure in HFSS is shown in Figure 14. In Figure 15, scattering parameters from our analytical method and HFSS are shown.

One may optimize the function $W(x)$ to obtain the best response.

These structures are easy to design and implement. They may find applications such as electromagnetic band-gap structures and DC

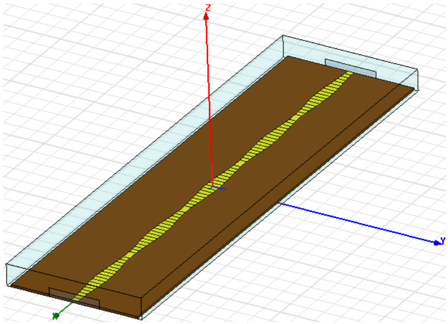

Figure 14. HFSS scheme of the periodic structure.

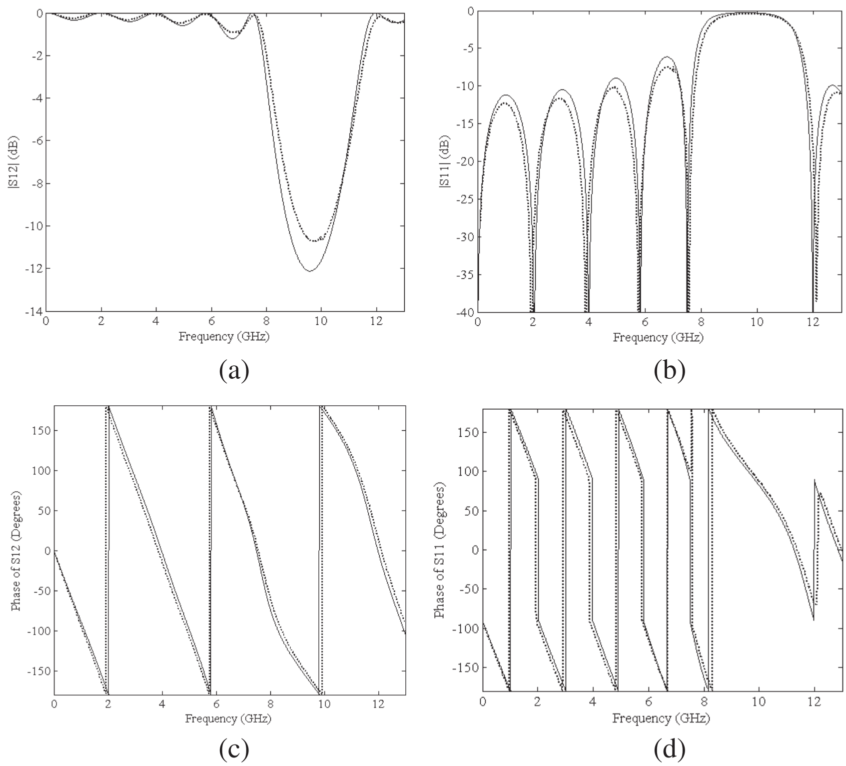

Figure 15. Scattering parameters (a) S_{12}, (b) S_{11}, (c) phase of S_{12}, (d) phase of S_{11} (…… HFSS, —— Analytical Method).

suppliers. In the stop band, the maximum rejection increases as the number of cells increases and it is calculated analytically and depicted in Figure 16.

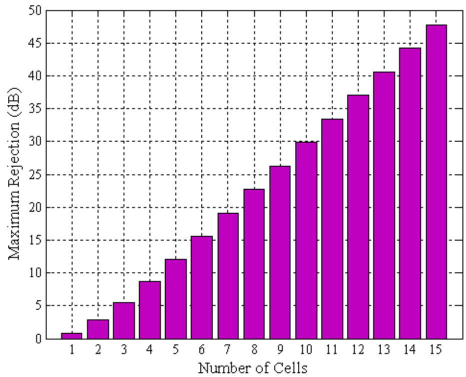

Figure 16. Maximum rejection in the stop band versus number of cells determined by the analytical method.

8. CONCLUSION

In this paper, a new method to design and analysis periodically loaded transmission lines, has been developed. Two novel parameters were introduced namely the *tardiness radius* and the *tardiness direction* which through them a simple form for the dispersion relation was deduced. The phase and the group velocities were derived with results to determine the phase reversal propagation and the anomalous dispersion conditions. It was shown that the bandwidth and the group velocity are inversely proportional to the tardiness radius. The tardiness direction helped us to determine the direction of phase velocity. Indeed, the strongest feature of the tardiness space is a fabulous insight which it gives into the phase and group velocities.

The other part of the paper was an atempt merely to show how the method works. A suggestion was made to construct and analyze symmetrical microstrip cells and a discussion was included to use these results to design a bandpass filter. A full wave simulation done by HFSS, verified the method.

ACKNOWLEDGMENT

The authors would like to thank Dr. K. Forooraghi for his advice during preparing this paper.

REFERENCES

1. Munk, B. A., *Frequency Selective Surfaces: Theory and Design*, John Wiley & Sons Inc., Apr. 2000.

2. Guo, C., H.-J. Sun, and X. Lv, "A novel dualband frequency selective surface with periodic cell perturbation," *Progress In Electromagnetics Research B*, Vol. 9, 137–149, 2008.
3. Hao, Y. and R. Mittra, *FDTD Modeling of Metamaterials: Theory and Applications*, Artech House, Inc., 2009.
4. Xie, H.-H., Y.-C. Jiao, K. Song, and Z. Zhang, "A novel multi-band electromagnetic band-gap structure," *Progress In Electromagnetics Research Letters*, Vol. 9, 67–74, 2009.
5. Pozar, D. M., *Microwave Engineering*, Addison-Wesley Publishing Company, 1990.
6. Caloz, C. and T. Itoh, *Electromagnetic Metamaterials: Transmission Line Theory and Microwave Applications, Engineering Approach*, John Wiley & Sons Inc., Nov. 2005.
7. Collin, R. E., *Foundations for Microwave Engineering*, McGraw Hill Inc., 1992.
8. Lu, W. B., T. J. Cui, X. X. Yin, Z. G. Qian, and W. Hong, "Fast algorithms for large-scale periodic structures using subentire domain basis functions," *IEEE Trans. Antennas Propag.*, Vol. 53, No. 3, 1154–1162, Mar. 2005.
9. Du, P., B. Z. Wang, and J. Deng, "An extended simplified sub-entire domain basis function method for finite-sized periodic structures," *Journal of Electromagnetic Waves and Applications*, Vol. 22, No. 11–12, 1479–1488, 2008.
10. Li, D. Y. and C. D. Sarris, "Efficient finite-difference time-domain modeling of driven periodic structures and related microwave circuit applications," *IEEE Trans. Microwave Theory Tech.*, Vol. 56, No. 8, 1928–1937, Aug. 2008.
11. Wu, Y. L., Y. X. Zhang, and Y. A. Liu, "Novel Smith chart approaches to solve problems in periodic structure," *International Conference on Microwave and Millimeter Wave Technology (ICMMT)*, Vol. 2, 605–608, Apr. 2008.
12. Jackson, J. D., *Classical Electromagnetics*, 3rd edition, John Wiley & Sons Inc., 1998.
13. Zandi, O., Z. Atlasbaf, and K. Forooraghi, "Flat multilayer dielectric reflector antennas," *Progress In Electromagnetics Research*, PIER 72, 1–19, 2007.
14. Mallick, A. K. and G. S. Sanyal, "Electromagnetic wave propagation in a rectangular waveguide with sinusoidally varying width," *IEEE Trans. Microwave Theory Tech.*, Vol. 26, No. 4, 243–249, Apr. 1978.